SAR Image Processing for Sea Surface Monitoring

B. Alpatov, O. Balashov, M. Ershov, V. Muraviev, A. Feldman
Department of Automation and Information Technologies in Control
Ryazan State Radio Engineering University, Ryazan, Russia
aitu@rsreu.ru

Abstract

Processing of SAR images are extensively used for control and monitoring of sea surface. Image data can be acquired from Earth observation satellites, such as TerraSAR-X, ERS, COSMO-SkyMed. Key areas of research include following the most relevant: detection of oil spills, detection of surface objects of artificial origin (ships and other vessels) and mapping of sea currents speed.

The paper describes several complex algorithms that solve these problems. The results of computer modeling on real SAR images are presented. Based on these results it is concluded that the proposed approaches can be used in practice.

Keywords: *SAR image, ship detection, oil spill detection, sea currents mapping.*

1. INTRODUCTION

It is known that about two-thirds of the Earth's surface is covered by water. Humanity is actively using ocean for freight shipping. Therefore, the tasks related to the monitoring of water surface are relevant. These tasks include ship detection, oil pollution control and sea currents research. Due to the fact that water surface covers wide areas, remote sensing is the most successful way of getting information about the ocean environment. Currently, the satellites equipped with synthetic aperture radar (SAR) antennas have received wide prevalence in solution of problems of water surface monitoring (TerraSAR-X, ERS-2, COSMO-SkyMed). The radar remote sensing satellites can obtain images of the ocean surface in any weather and any time.

2. OIL SPILL DETECTION

Mass use of petroleum products around the world creates preconditions for increasing volumes of production of crude oil and transportation of petroleum products. This increases the probability of water surface pollution. Problem of ecological monitoring of marine environment gets more acuity; thereby the development of oil spill detection algorithm is an important task [7].

2.1. Radar imaging and oil slicks

Radio waves are sensitive to the state of the sea surface because wind waves are present on it. Reflection mechanism of radio waves from such surface is described by the Bragg scattering [8]. Oil pollution inhibits the interaction of wind with the water surface. Due to this effect, the scattering of radio waves decreases in the antenna direction (Figure 1).

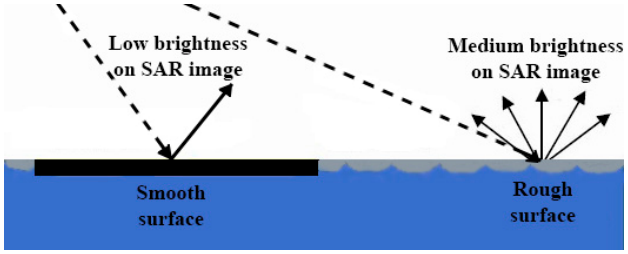

Fig. 1. Scattering of radio waves from the sea surface

2.2. Oil spill detection algorithm

A SAR image $l(m,n)$ presented by grayscale image is input data for the oil spills detection algorithm. The algorithm consists of the following main steps: image preprocessing, detection of dark segments, parameter extraction and classification of detected dark segments.

2.2.1. Image preprocessing

Preprocessing may consist of two parts: filtering of a speckle noise and masking of land areas.

The speckle noise is an integral component of the SAR image and can significantly affect the results of processing. So we can use mean, median, adaptive Lee, Frost filters or other filters to reduce the noise of images.

As the area of interest is water surface, the second step of the preprocessing is masking of land areas (Figure 2). This preprocessing step leads to the avoidance of false detections which are associated with relief roughness and other features of the land surface. For this purpose, the vector database of coastlines is used.

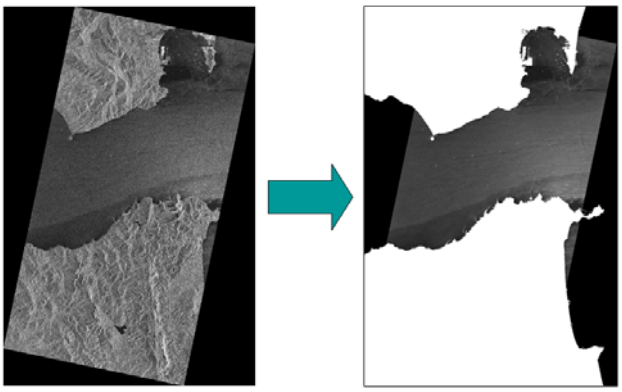

Fig. 2. Example of land masking

2.2.2. Detection of dark segments

An important step of the algorithm is detection of dark spots in the processing image. Segmentation is performed in order to pick out the dark areas which generally correspond to oil pollution. An adaptive threshold filtering is performed at this stage of the oil spill detection algorithm. This filtering is based on an estimate of roughness of the surrounding sea surface and consists of the following steps:

1. The mean value $\mu(m,n)$ and the standard deviation of brightness $\sigma(m,n)$ are computed in local window with size $w \times w$ for each pixel of the image $l(m,n)$, according to (1) and (2):

$$\mu(m,n) = \frac{1}{(w+1)^2} \sum_{x=m-w/2}^{m+w/2} \sum_{y=n-w/2}^{n+w/2} l(x,y), \quad (1)$$

$$\sigma(m,n) = \sqrt{\frac{1}{(w+1)^2 - 1} \sum_{x=m-w/2}^{m+w/2} \sum_{y=n-w/2}^{n+w/2} \left(l(x,y) - \mu(m,n)\right)^2}. \quad (2)$$

2. Calculation expression $\lambda(m,n)=\frac{\sigma(m,n)}{\mu(m,n)}$ for each pixel of the image $l(m,n)$. Homogeneity category K is determined in accordance with the calculated value $\lambda(m,n)$ in a neighborhood of the point (m,n).

3. Calculation of the threshold value $T(m,n)=\frac{\mu(m,n)}{d(K)}$. The coefficient $d(K)$ is selected from a premade table according to a certain category of homogeneity.

4. Obtaining of the binary image $b(m,n)$ by thresholding according to expression

$$b(m,n)=\begin{cases}1, \text{ if } l(m,n)\geq T(m,n);\\ 0, \text{ otherwise.}\end{cases} \quad (3)$$

2.2.3. Parameter extraction from detected dark segments

Marking and parameterization of the binary image is performed after the detection of dark spots. As a result of this operation, all connected regions in the image are combined into individual segments. A set of parameters is determined for each segment: area S, perimeter P, coordinates of the segment's center, circularity c, eccentricity ε and others.

The marking and parameterization algorithm of the binary image $b(m,n)$ is performed by adding a label matrix Q and line by line image processing. We assume that the white points are part of objects – the oil spills and the black points are part of background – the sea surface.

2.2.4. Classification

Dark segments classification is an important step of the oil spill detection algorithm and requires a complex estimation of each segment. The set of slicks that are likely oil spills are formed at this stage.

One of the main features that characterize the oil pollution is its geometric shape which is determined by the circularity and the eccentricity. Other important parameter of the oil slick is its size. Segments having too small area are likely formed due to the strong sea surface disturbance and the interference effects. Too large segments are usually slicks of natural origin (colonies of algae) or calm areas. Edge detection of pollution areas plays an important role because oil spills typically have a well-defined smooth contour. Moreover, distinctive feature of oil slicks from natural pollution is the homogeneity of their texture.

3. SHIP DETECTION

One of the important problems arising in the field of SAR images interpretation is the detection of ships and vessels of various classes. Ship detection is a crucial application for global environmental monitoring and security. This allows to monitor traffic, fisheries and to associate ships with oil discharge.

Although the objects in the image are clearly visible, the presence of intense noise and clutter makes the problem of detection much more difficult. To improve the obtained results a reliable and fail-safe approach should be developed. Ship detection algorithm proposed in this paper consists of the following main stages: prescreening, land masking, image segmentation combined with parameter measurement, ship orientation estimation and size correction, object discrimination.

Prescreening involves the processing of the original SAR image using a multi-window averaging filter followed by adaptive local thresholding. The small window of size $w_s \times w_s$ is constructed in the neighborhood of the current pixel (m,n) and the local average $\overline{\mu}_s(m,n)$ is calculated. The window is used to smooth the noise and to find a more accurate estimate of the object brightness. For the pixel under test the background statistics is estimated in the region bounded by window of size $w_s \times w_s$ on the one side and the filtering window of $w_b \times w_b, w_b >> w_s$ size on the other side (Figure 3). It is assumed that the background in local region can be approximated by the normal distribution with $\mu_b(m,n)$ mean and variance $\sigma_b^2(m,n)$. All windows are moved one pixel at a time across the whole image.

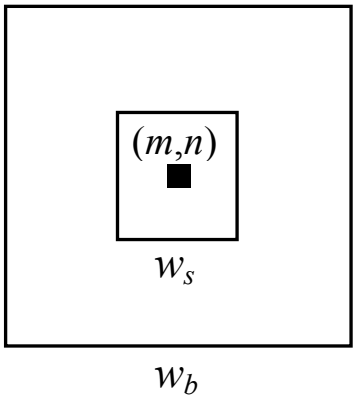

Fig. 3. Window setup for filtering

A binary image is obtained according to the rule (4):

$$b(m,n)=\begin{cases}1, \text{ if } \overline{\mu}_s(m,n) > \overline{\mu_b}(m,n)+\overline{\sigma_b}(m,n)\, t / w_s,\\ 0, \text{ otherwise,}\end{cases} \quad (4)$$

where $\overline{\mu}_b(m,n)$, $\overline{\sigma}_b(m,n)$ – background average and standard deviation, t – threshold. The exact value t is chosen based on a given probability of false alarms $P_{fa}=0{,}5-0{,}5erf(t/\sqrt{2})$, where $erf(...)$ is the error function. In a binary image nonzero pixels belong to objects and others to background. At this stage the land mask can be implemented to allocate areas that don't contain sea surface. The described approach is similar to the CFAR detector, which is widely used in practice [2, 3].

However, the extended objects may be fragmented in the binary image, which leads to incorrect ship parameters estimation. Therefore, to increase the reliability of the algorithm an image segmentation stage is suggested for object mask restoration purposes.

Region growth algorithm is used as a basis for image segmentation. In the process of line by line scanning of image $b(m,n)$ the first pixel with nonzero value is treated as the start position for subsequent region growth. Then the neighboring pixels are viewed in the original SAR image.

It is considered that the analyzed point belongs to the segment, if it satisfies the homogeneity criterion $|l(m,n)-\mu_l|<T_l$, where $l(m,n)$ is the brightness of the analyzed pixel in the original image, μ_l – the average brightness of the segment, T_l – the predetermined threshold. To improve binding for all pixels that belongs to original mask no checks are performed. If a new pixel is added to the segment, its area S and average brightness μ_l are recalculated.

This process continues as long as a segment increases in its size also taking into account the connectivity conditions. Thus the form of the segment can be recovered and such parameters as

area, average brightness and bounding box can be simultaneously estimated.

With a restored object binary mask the corresponding pixels values in image $b(m,n)$ are set to zero. After that the searching of remaining nonzero pixels in $b(m,n)$ continues. If such pixel is found then the region growth algorithm is started in the new start position. Segmentation stage terminates at the end of the search procedure.

For correct ship size measurement it is important to accurately estimate its orientation. For a connected region R, which describes the binary segment mask, central moments of the second degree by row μ_{nn}, column μ_{mm} and a mixed central moment μ_{mn} are evaluated (5):

$$\mu_{mm} = \sum_{(m,n)\in R}(m-m_c)^2/S\ ,\ \mu_{nn} = \sum_{(m,n)\in R}(n-n_c)^2/S\ ,$$

$$\mu_{mn} = \sum_{(m,n)\in R}(m-m_c)(n-n_c)/S\ , \qquad (5)$$

where (m_c, n_c) is the region centroid. Usually the object corresponding to the ship has a well distinguishable principal axis. It is understandable that the orientation of a ship is actually the direction of its principal axis with angle $\alpha = \frac{1}{2} arctg\left(2\mu_{mn}/(\mu_{nn}-\mu_{mm})\right)$.

Object discrimination is the rejection of false alarms using object parameters analysis. Typically the width-to-length ratio of a ship lies in the range from 1/10 to 1/7 [8].

As the satellite image resolution is known the maximum and minimum area of a ship in meters can be simply converted to pixels. Objects with inappropriate area and aspect ratio are excluded from consideration. When all the required checks are made the list of final object parameters includes center, orientation, size and average brightness.

4. MEASUREMENT OF THE SEA CURRENTS SPEED

Sea currents allow track processes in the oceans. The described algorithm is designed to measure speed of sea currents. The result of the algorithm is a contour map of the speed of sea currents.

To measure sea currents information about the amplitude and phase of the reflected signal is required [1]. To find the solution of a considered task it is necessary to use SAR images such as images of SSC level processing, obtained by the spacecraft TerraSAR-X.

Suppose that we have SAR image of the sea surface, containing information about the amplitude and phase of the reflected signal. The process of mapping of sea surface speed can be described as follows. It is known that according to Doppler's law the frequency of the reflected signal changes in proportion to the object speed. Therefore, movement of the water surface (horizontal movement) as a part of the sea current affects the formation of SAR images [4, 5].

Sea currents have an influence on the satellite speed relative to the ocean surface. Due to the Doppler effect, the frequency f_{DC} of the reflected signal changes to the value

$$f_{DCA} = f_{DC} - f_{DCM}, \qquad (6)$$

where f_{DCM} is the frequency of the reflected signal for the case of no sea currents [1]. For the TerraSAR-X image the frequency f_{DCM} can be computed from the data stored in the image passport file [6] using the expression $f_{DCM} = k_0 + k_1 t$, where t is the period of a signal passing from the beginning to the current point of the image, k_0, k_1 – coefficients stored in the image passport file.

The SAR image data allow us to measure the Doppler centroid f_{DC}. The Doppler shift is calculated using the expression (6). Sea current radial velocity is evaluated from [4]

$$V_D = -\frac{\pi f_{DCA}}{k_R \sin\theta}\ , \qquad (7)$$

where V_D – projection of an object's speed to the observation direction; θ – the incidence angle; $k_R = 2\pi/\lambda$; λ – the wavelength of the SAR-radar. The final expression for the sea current speed is obtained from (7), thus

$$V = V_D \sin\theta \cos\psi\ , \qquad (8)$$

where ψ is the angle between the observation plane and the water flow direction.

5. EXPERIMENTAL RESULTS

The SAR images obtained from remote sensing satellites TerraSAR-X, ERS-2 were used as the input data for experiments.

The result of the oil spill detection algorithm is shown in Figure 4. Spots classified as oil spills are outlined by rectangles. Size of these spills is displayed in square kilometers.

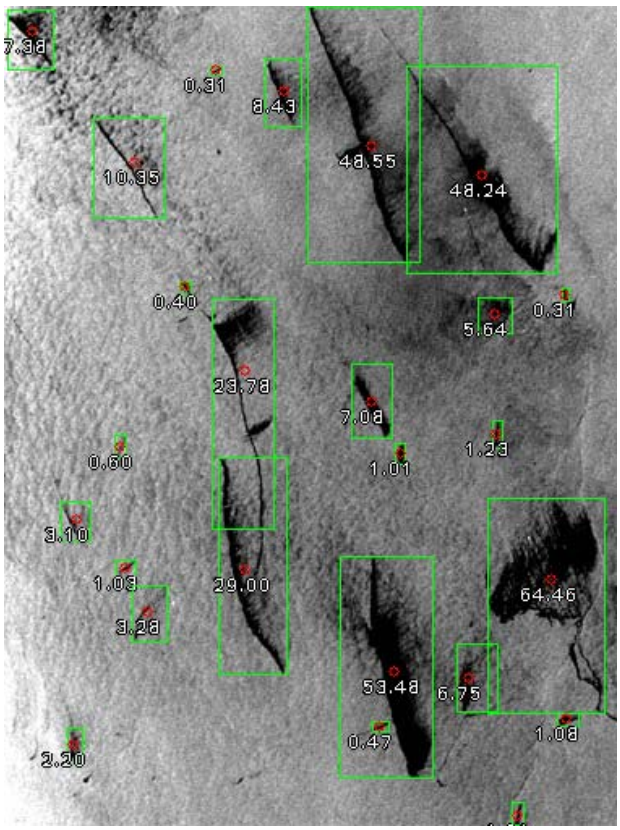

Fig. 4. Result of oil spills detection in SAR image

The result of the ship detection algorithm is shown in Figure 5. Objects of interest are marked by ellipses.

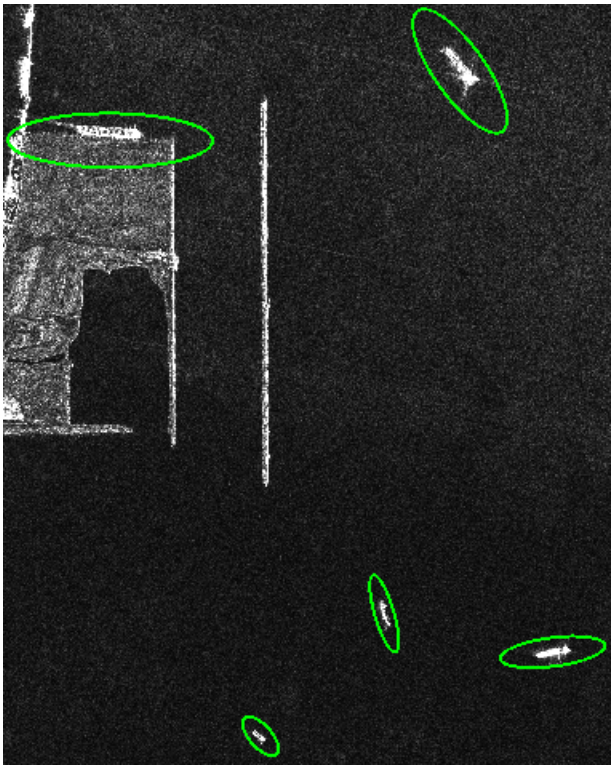

Fig. 5. The result of ship detection

6. CONCLUSION

This paper describes the developed algorithms of SAR image processing. The proposed approaches are modeled on the real TerraSAR and ERS-2 images. Presented algorithms are focused to solve a number of important scientific and practical tasks, including control of illegal fishing, ocean pollution, discovery of new oil deposits, studies of phytoplankton life, mapping of sea currents.

In practice the algorithms can be used for:

- high-precision measurement of ship characteristics and parameters;

- measurement of spills characteristics on the sea surface;

- distinguishing spills, formed by both artificial and natural pollutions;

- studies of surface masses movement.

Thus, the developed algorithms can be used as a very efficient tool for sea surface monitoring.

7. ACKNOWLEDGMENTS

This work was supported by grant RFMEFI57414X0056 from the Ministry of Education and Science of the Russian Federation.

8. REFERENCES

[1] Chapron B., Fabrice C., Fabrice A. Direct Measurements of Ocean Surface Velocity from Space: Interpretation and Validation. Journal of Geophysical Research, 2005, Vol. 110. – P. 1 – 17.

[2] Hinz S., Meyer F. Automatic ship detection in space-borne SAR imagery // International Archives of Photogrammetry, Remote Sensing and Spatial Information Sciences, 2009, Vol. 38. – 6 p.

[3] Jiayuan L., Mingzhu L., Shuhong J. An adaptive ship detection method in SAR image based on CFAR // 2nd International Conference on Information Communication and Management, Singapore, 2012, Vol. 55. – P. 51 - 55.

[4] Johannessen J.A., Kudryavtsev V., Chapron B., Collard F., Akimov D., Dagestad K.-F. Backscatter and Doppler signals of surface current in SAR images: a step towards inverse modeling. Proceedings of SEASAR 2006, 23 - 26 January 2006, Frascati, Italy.

[5] Kang M., Lee H. Estimation of Ocean Current Velocity near Incheon using Radarsat-1 SAR and HF-radar Data. Korean Journal of Remote Sensing, 2007, Vol. 23, No. 5. – P. 421 - 430.

[6] TerraSAR-X Ground Segment Level 1b Product Format Specification. 2007. – P. 257.

[7] Topouzelis K.N. Oil Spill Detection by SAR Images: Dark Formation Detection, Feature Extraction and Classification Algorithms. Journal Sensors, 2008, Vol. 8. –P. 6642 - 6659.

[8] Verba V.S., Neronskiy L.B., Osipov I.G., Turuk V.E. Spaceborne Earth Surveillance Radar Systems. – M.: Radiotechnika, 2010. – 681 p., in Russian.

About the authors

Alpatov Boris (D.Sc.Tech.) is a professor, head of Department of Automation and Information Technologies in Control (DoAITC), Ryazan State Radio Engineering University (RSREU).

Balashov Oleg (Ph.D.) is an associate professor at DoAITC, RSREU.

Ershov Maksim is an engineer at DoAITC, RSREU.

Muraviev Vadim (Ph.D.) is an associate professor at DoAITC, RSREU.

Feldman Alexander (Ph.D.) is an assistant researcher at DoAITC, RSREU.